BIOCHEMISTRY
including biophysical chemistry & molecular biology
Article

Biochemistry **2009,** *48,* 5839–5848 5839
DOI: 10.1021/bi802309y

DevS Oxy Complex Stability Identifies This Heme Protein as a Gas Sensor in *Mycobacterium tuberculosis* Dormancy†

Alexandra Ioanoviciu,‡ Yergalem T. Meharenna,§ Thomas L. Poulos,§ and Paul R. Ortiz de Montellano*,‡

‡*Department of Pharmaceutical Chemistry, University of California, 600 16th Street, San Francisco, California 94158-2517, and* §*Departments of Molecular Biology and Biochemistry, Chemistry, and Pharmaceutical Sciences, University of California, Irvine, California 92697-3900*

Received December 18, 2008; Revised Manuscript Received May 19, 2009

ABSTRACT: DevS is one of the two sensing kinases responsible for DevR activation and the subsequent entry of *Mycobacterium tuberculosis* into dormancy. Full-length wild-type DevS forms a stable oxy−ferrous complex. The DevS autoxidation rates are extremely low (half-lives of >24 h) in the presence of cations such as K^+, Na^+, Mg^{2+}, and Ca^{2+}. At relatively high concentrations (100 mM), Cu^{2+} accelerates autoxidation more than 1500-fold. Contrary to expectations, removal of the key hydrogen bond between the iron-coordinated oxygen and Tyr171 in the Y171F mutant provides a protein of comparable stability to autoxidation and similar oxygen dissociation rate. This correlates with our earlier finding that the Y171F mutant and wild-type kinase activities are similarly regulated by the binding of oxygen: namely, the ferrous five-coordinate complex is active, whereas the oxy−ferrous six-coordinate species is inactive. Our results indicate that DevS is a gas sensor in vivo rather than a redox sensor and that the stability of its ferrous−oxy complex is enhanced by interdomain interactions.

Tuberculosis remains a health concern in the 21st Century, as it is a leading cause of mortality among infectious diseases and results in the death of 2−3 million people each year (*1*). Active tuberculosis cases are recruited from an immense reservoir of ~2 billion people latently infected with the bacillus worldwide (*1*, *2*). Despite the magnitude of this health problem, no new drug has been introduced for tuberculosis therapy over the past 30 years. The current tuberculosis treatment requires at least 6 months, which makes it costly and reduces patient compliance. The available medications can be used with only limited success in infections caused by the rapidly emerging resistant tuberculosis strains, particularly multidrug resistant and extensively drug resistant tuberculosis (*3*). Latent tuberculosis is itself very difficult to treat, since dormant *Mycobacterium tuberculosis* displays a diminished susceptibility to drugs.

The mechanism of the entrance of *M. tuberculosis* into the dormant phase still needs to be unraveled (*4*); this is a key step in the development of new and more effective approaches to the therapy of this disease. When *M. tuberculosis* enters dormancy, it alters its metabolism in response to unfavorable environmental stimuli and undergoes striking morphological changes (*5*, *6*). Dormant *M. tuberculosis* bacilli have a thicker modified cell wall (*7*) that has lost its acid-fastedness and is Ziehl−Neelsen negative (*8*, *9*). HspX (Rv2031), an α-crystallin-like heat shock protein upregulated in this phase (*10*, *11*), is, in fact, one of the most abundant proteins in dormant bacilli (*11*). Rv2031 belongs to the "dormancy regulon" (*12*, *13*), a set of 48 genes whose expression is induced upon entry of *M. tuberculosis* into the dormant state. α-Crystallin performs a key function in *M. tuberculosis*: it maintains proteins in their functional form and thus reduces the need for the de novo biosynthesis of proteins required for bacterial survival (*10*, *11*).

Induction of the dormancy regulon is accomplished exclusively via the DevS/DosT/DevR two-component system. DevS and DosT are the only sensing kinases within the *M. tuberculosis* genome that are capable of activating DevR (*14*). Both kinases are heme proteins that bind oxygen, nitric oxide, and carbon monoxide, the very stimuli that determine whether *M. tuberculosis* will enter the dormant state. The identification of DevR protein in *M. tuberculosis* inside in vitro infected human monocytes (*15*) suggests that the DevS/DosT/DevR transduction pathway is operational in vivo and is clinically relevant. Interestingly, antibodies against HspX are frequently identified in tuberculosis patients (*16*), providing further support for the relevance of a functional DevS/DosT/DevR system in human tuberculosis infections.

So far, DevS and DosT appear to be redundant in their function, suggesting that *M. tuberculosis* needs multiple genes to ensure that this important transduction system is functional. A difference that has been noted, however, is differential induction of protein expression in response to hypoxia: DevS expression is induced by hypoxia, whereas DosT expression is not (*17*). Recent reports have also suggested that the two proteins may display different stabilities of the oxy complexes (*18*−*20*). DevS and

†This work was supported by Grants AI074824 (P.R.O.d.M.) and GM42614 (T.L.P.) from the National Institutes of Health.

*To whom correspondence should be addressed: University of California, Genentech Hall GH-N572D, 600 16th St., Box 2280, San Francisco, CA 94158-2517. Telephone: (415) 476-2903. Fax: (415) 502-4728. E-mail: ortiz@cgl.ucsf.edu.

Published on Web 05/22/2009

DosT are highly homologous, and both possess a heme moiety anchored to the N-terminal GAF domain. The facile oxidation of the oxy−DevS complex as compared to DosT in the hands of Kumar et al. (*19*) and Cho et al. (*20*) led the authors to propose that DevS is a redox sensor while DosT is a gas sensor. In contrast, the two proteins have also been reported to have similar low autoxidation rates (*18*). A discrepancy thus exists in the reported autoxidation rate for DevS and, consequently, in our understanding of its physiological function.

We have performed a detailed study of full-length wild-type DevS autoxidation in an effort to understand the role of DevS in vivo as well as the factors that may contribute to its stability and lability to autoxidation. We compare full-length DevS to its truncated versions and to the full-length Y171F DevS mutant. Tyr171 is hypothesized to assist in signal transduction and to stabilize the oxy complex by donating a hydrogen bond to the oxygen molecule that coordinates to the ferrous heme iron.

MATERIALS AND METHODS

Chemicals (≥99.999% pure metal salts) were purchased from Sigma Aldrich. Ampicillin was purchased from Fisher Biotech, while chloramphenicol was obtained from Roche, hemin from Fluka Biochemica, dithionite from J. T. Baker, and IPTG[1] from Promega. Lysozyme and phenylmethanesulfonyl fluoride were from Sigma. Protease inhibitors (antipain, leupeptin, and pepstatin) were obtained from Roche.

Protein Expression and Purification. Genetic manipulations were performed, and recombinant proteins were expressed and purified as described in our previous publications (*21*−*23*).

General Procedure for Autoxidation Reactions. The protein sample was reduced inside a glovebox with excess dithionite (100 mM solution) and then desalted on a PD10 column. All tubes and glassware were first rinsed with a 5 mM dithionite solution and then five times with anaerobic buffer. The protein sample (600 μL) was removed from the glovebox in an anaerobic cuvette, and the starting spectrum was recorded. Then oxygenated buffer was added (250−600 μL), and UV−visible spectra were typically recorded for 1−3 days at 15 min time intervals. The data obtained were analyzed with Specfit and fitted to the single-exponential model reaction A converted to B. The starting and ending spectra of DevS were used as limits for the fitting procedure. Two types of buffers were used: either 20 mM Hepes (pH 7.5), pretreated with Chelex 100 resin, or 50 mM phosphate buffer (pH 7.5) containing 200 mM NaCl and 1 mM EDTA. If Hepes buffer treated with Chelex was used, the protein sample was treated with EDTA before the desalting step. Reagents of high purity (≥99.999%) were used to determine the effect of metal ions on autoxidation rates. Autoxidation rate measurements were conducted at 25 °C in duplicate.

Reduction of Full-Length DevS. Ferric full-length DevS was reduced by ferredoxin (Rv0763c) and ferredoxin reductase (Rv0688) under anaerobic conditions to the ferrous form. These reductase proteins were provided by H. Ouellet (University of California, San Francisco, CA). Full-length DevS was fully oxidized inside the glovebox using ferricyanide to the ferric form, and it was desalted on a PD10 column to transfer it to 20 mM Hepes buffer containing 1 mM EDTA. The final protein concentration was 2.5 μM. Ferredoxin was then added to a final concentration of 5 μM, and ferredoxin reductase was present at a concentration of 1 μM. The final NADH concentration was 100 μM. Glucose oxidase (2 units/mL), glucose (10 mM), and catalase (100 μg/mL) were also added to ensure complete removal of oxygen traces. The ferredoxin/ferredoxin reductase combination was added to the DevS protein sample; the solution was mixed quickly in the 500 μL cuvette, and then spectra were recorded every 30 s for 30 min. The data were fit to the first-order rate equation by monitoring the absorbance changes at the two wavelengths (405 and 433 nm) where changes were maximal, as established from the difference spectrum between the ferric and oxy−ferrous DevS complex. The data from 150 s onward were fit to the single-exponential equation to yield the reduction reaction rates. This experiment was conducted three times, and the results were averaged.

Stopped-Flow Experiments and Determination of Kinetic Constants of Ligand Binding. Kinetic parameters were measured using a Hi-Tech KinetAsyst Stopped Flow System (SF-61DX2) in diode array mode, with some experiments repeated in photomultiplier mode at the wavelength of maximal spectral change. CO binding constants were determined at 4 °C, while oxygen dissociation rates were measured at 25 °C. Data sets were analyzed using Specfit (version 3.0.36 for 32 bit Windows systems). Each data point represents the average of five or six independent determinations. All kinetic experiments were performed at least three times.

Phosphate buffer (50 mM, pH 7.5) containing 200 mM NaCl and 1 mM EDTA was used for all solutions. Heme protein concentrations were in the range 3−7 μM. Protein samples were typically reduced with excess dithionite inside the anaerobic glovebox and desalted on PD10 columns. The oxy complexes were prepared by mixing the reduced protein sample with aerated buffer, while CO complexes were formed by adding CO-saturated buffer to the ferrous species to a final concentration of 50 μM. Ligand solutions were prepared in gas-tight syringes under anaerobic conditions inside a glovebox from saturated CO and NO buffers.

For the determination of CO association constants, ligand concentrations ranged from 50 to 250 μM. Generally, the k_{obs} (s^{-1}) was determined at seven different concentrations and plotted as a function of ligand concentration (μM); the slope provided the CO association constant.

The CO dissociation constant was measured using the wild-type DevS−CO complex and air-saturated buffer. The result was confirmed using 80% air-saturated buffer, 100% NO, and 80% NO saturated solutions. The CO dissociation constant for the DevS Y171F mutant was determined using NO solutions (80 and 100% saturated).

Oxygen dissociation rates were measured using CO-saturated solutions for the wild-type DevS protein constructs, while dithionite solutions (5 and 6 mM) were used in the case of Y171F DevS.

Laser-Flash Photolysis Experiments. Oxygen association rates were measured using laser-flash photolysis with a pulsed dye laser system fitted with a Quantel Brilliant B Nd:YAG laser. Solutions were irradiated at 540 nm with a pulse of 10 ns and monitored at 434 nm. Formation of the complex was confirmed by optical absorption spectra recorded before and after laser-flash photolysis measurements. In the case of both wild-type DevS and the Y171F mutant, the ferric heme was first reduced

[1]Abbreviations: IPTG, isopropyl β-D-thiogalactopyranoside; wt, wild-type; GAF domain, protein domain conserved in cyclic GMP-specific and stimulated phosphodiesterases, adenylate cyclases, and *Escherichia coli* formate hydrogenlyase transcriptional activator (Pfam accession number PF01590).

with sodium dithionite in deoxygenated buffer. Then, the excess dithionite was removed by loading the sample onto a column of Sephadex G-25 and the protein sample was eluted with buffer containing known oxygen concentrations. The oxygen stock solution was prepared by equilibrating the buffer with 1 atm of pure oxygen gas at room temperature. All of the kinetic measurements were conducted at pH 7.5 in phosphate buffer (20 mM) containing 200 mM NaCl and 1 mM EDTA.

RESULTS

The autoxidation rates of ferrous oxygen-bound complexes are widely considered a key parameter that reflects the stability of heme proteins (*24*, *25*). In this work, we have examined the autoxidation of full-length DevS over extended periods of time at room temperature in the presence and absence of metal ions. In addition, we have investigated the autoxidation behavior of the isolated GAF A domain, GAF A/B domains, and Y171F full-length mutant to investigate the influence of the protein context on the autoxidation rates.

The heme proteins used in this study were coexpressed with the GroEL/ES chaperones as previously reported to promote protein folding (*21*). This is a key step, as it is the protein matrix that protects the heme from oxidation (*26*). Minimal changes in the distal pocket that affect the size and hydrophobicity of the heme environment have been shown to modulate the stability of the corresponding oxy complexes (*26*−*28*). To this end, site-directed mutagenesis experiments, mainly conducted with myoglobins, have demonstrated that the shape, size, and lipophilicity of the heme pocket modulate resistance to autoxidation. These earlier results show that the protein architecture is of prime importance and may account for the discrepancy in the previously published results on DevS autoxidation (*18*, *19*).

The degradation of the full-length DevS−oxy complex to the met form upon exposure to air was monitored by UV−vis spectroscopy. In buffers free of transition metals, DevS proved to be very stable to autoxidation (Table 1). The conversion of the oxy complex to the ferric form is extremely slow in phosphate buffer in the presence of 1 mM EDTA or in 20 mM Hepes buffer pretreated with Chelex, with $t_{1/2}$ values of >30 h. Removal of transition metal ions either by using a cation exchange resin (Chelex 100) or by sequestration as an inert EDTA chelate provides an environment in which the oxy−DevS complex is highly stable. Mg^{2+} and Ca^{2+} ions are commonly used by kinases, and DevS requires Mg^{2+} for autophosphorylation (*17*, *29*). Neither Ca^{2+} (0.1 mM) nor Mg^{2+} (1 mM) accelerated the autoxidation of full-length DevS. We next examined the stability of DevS in the presence of 200 mM KCl or 200 mM NaCl. Again DevS was very resistant to autoxidation. We then selected two ions found in biological fluids at low concentrations, Fe^{3+} and Cu^{2+}. In the presence of 0.1 mM Fe^{3+}, the autoxidation of DevS was mildly accelerated (half-life of 7.8 h). Interestingly, addition of 0.1 mM Cu^{2+} resulted in a large enhancement of the autoxidation rate from more than 60 h to less than 2 min. We conclude that DevS displays a very high stability to autoxidation in the presence of physiologically relevant cations such as Na^+, K^+, Mg^{2+}, and Ca^{2+}, but Cu^{2+} at relatively high concentrations is able to act as an efficient electron acceptor and oxidizes the oxy−DevS complex at high rates ($k = 25\ h^{-1}$). The stability of the oxy−DevS complex to autoxidation suggests that DevS functions as a gas sensor in vivo. Autoxidation is very slow, characterized by half-lives greater than 1 day in the absence of Fe^{3+} and Cu^{2+}. The physiological concentrations of iron and copper are very low compared to the levels tested in this study and therefore are unlikely to cause a significant acceleration of DevS autoxidation. We note that a 10-fold decrease in Cu^{2+} concentration (from 100 to 10 μM) decreased the DevS autoxidation rate more than 300-fold and correspondingly increased the autoxidation half-life from less than 2 min to 11 h. We conclude that the oxy−DevS complex is very stable in the mycobacterial cell.

Table 1: Autoxidation Rates of Full-Length Wild-Type DevS in the Presence of Common Metal Ions[a]

conditions	k (h^{-1})	$t_{1/2}$ (h)
200 mM KCl[b]	0.013	78
0.1 mM $CaCl_2$[b]	0.0049	170
1 mM $MgCl_2$[b]	0.012	59
200 mM NaCl[b]	0.010	96
20 mM Hepes[b]	0.0033	210
phosphate EDTA[c]	0.019	36
0.1 mM $CuCl_2$[b]	25	0.03
10 μM $CuCl_2$[b]	0.062	11
0.1 mM $FeCl_3$[b,d]	0.089	7.8

[a] Rates were measured at 25 °C. [b] In Hepes buffer (20 mM, pH 7.5), pretreated with Chelex 100 resin. The cations indicated were added as salts of high purity (≥99.999%). [c] In phosphate buffer (50 mM, pH 7.5), 1 mM EDTA, and 200 mM NaCl. [d] The nominal $FeCl_3$ concentration is indicated.

Representative traces of autoxidation experiments are shown in Figures 1 and 2. In Figure 1, a three-dimensional plot of UV−visible spectra collected over time shows that the oxy−DevS complex is very slowly converted to ferric DevS in the presence of 200 mM NaCl over the course of roughly 3 days. In Figure 2, DevS quickly undergoes autoxidation from the oxy form to the ferric complex in the presence of Cu^{2+}. In this experiment, spectroscopic traces were collected every 30 s for a total of 8 h (only traces from the first 30 min of the experiment are shown). Clear isosbestic points at 413, 524, 594, and 648 nm indicate that a smooth conversion occurs from the oxy complex reactant into the product met form under these conditions.

Next we compared full-length wild-type DevS to the truncated proteins GAF A DevS and GAF A/B DevS in phosphate buffer containing EDTA (Table 2). The first of these proteins consists only of the heme-containing GAF A domain and the second of the GAF A and B domains. All the proteins are fairly stable to autoxidation under these conditions. GAF A DevS is the least stable (half-life of 16.5 h) followed by GAF A/B DevS (half-life of 26.0 h). Full-length Y171F DevS (half-life of 73.6 h) is the most stable in this series.

The autoxidation behavior of Y171F is similar to that of wild-type full-length DevS (Table 2).

Heme proteins used for oxygen storage and transportation are physiologically active only in the ferrous form and autoxidize spontaneously to the inactive met form. Reduction systems are normally present to reduce the ferric forms back to the ferrous complexes that are capable of binding oxygen. For this reason, we have examined the reduction of full-length DevS by an endogenous *M. tuberculosis* ferredoxin reductase/ferredoxin system, the Rv0688 and Rv0763c gene products, respectively. As shown in Figures S1 and S2 of the Supporting Information, ferric full-length DevS was quickly reduced by this system to the ferrous form, at a rate of 0.0027 s^{-1}, as monitored at both 405 and 433 nm ($t_{1/2}$ = 4.4 min). We propose that DevS, if oxidized to met-DevS, can be reduced inside *M. tuberculosis* to the physiologically relevant ferrous DevS, the active kinase.

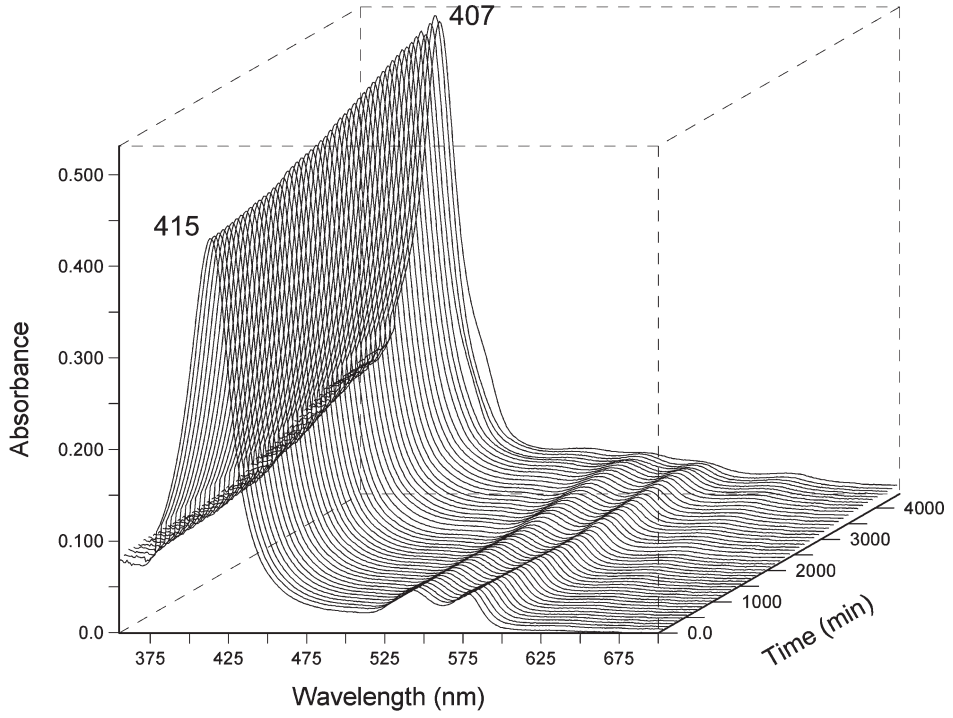

FIGURE 1: Autoxidation of wild-type full-length DevS in the presence of 200 mM NaCl and 20 mM Hepes buffer (pH 7.5) at 25 °C. The reaction was monitored every 15 min for 3 days. Other metal ions were excluded using a Chelex 100 anion exchange resin.

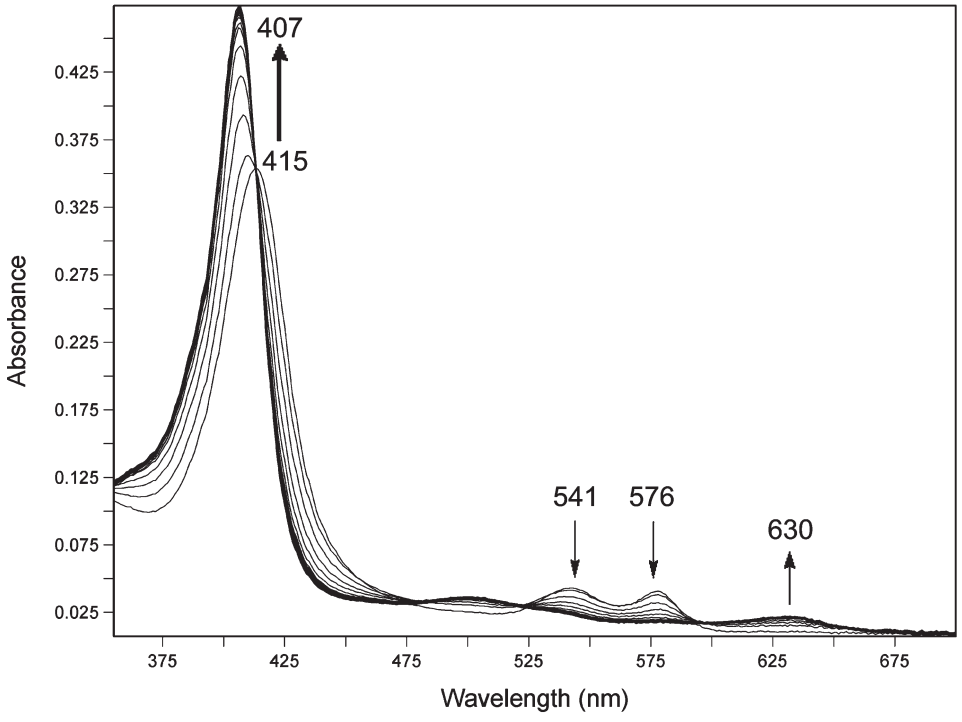

FIGURE 2: Autoxidation of wild-type full-length DevS in the presence of 100 μM $CuCl_2$ and 20 mM Hepes buffer (pH 7.5) at 25 °C. The reaction was monitored every 30 s for 8 h. Only 50 spectra recorded during the first half-hour of the experiment are shown. Other metal ions were excluded using a Chelex 100 anion exchange resin.

Kinetic CO and O_2 binding parameters were determined for wild-type DevS and Y171F DevS (Figure 3). Additionally, CO association and dissociation constants were measured for the truncated DevS constructs. While the differences in CO on rates are small, ranging from 0.18 to 0.73 μM^{-1} s^{-1}, a clear trend is established; CO association constants increase in the following order: DevS A GAF < DevS A/B GAF < DevS < Y171F DevS. Representative traces of CO binding to Y171F DevS are shown in Figure 3. The CO k_{on} for wild-type DevS proteins is higher than for FixL gas sensors, including BjFixL (0.005 μM^{-1} s^{-1}) (*30*), and comparable to the CO association rate of the AxPHEA heme domain (*31*).

CO off rates are virtually constant in the DevS protein series at ~2.5 s^{-1}, and notably higher than CO off values for FixLs. UV−visible spectra of the displacement reaction between Y171F

Fe^{2+} CO and NO are included in Figure 4. These trends result in an increase in K_{DCO} in the following order: Y171F DevS < DevS < DevS A/B GAF < DevS A GAF. Wild-type full-length DevS has a K_{DCO} value that is quite close to the BjFixL constant (9 μM) (*30*).

The oxygen association constant for the Y171F mutant is ~3 times larger than that of the wild type (Table 3). The wild-type DevS value is lower, while the mutant O_2 association constant is higher than the corresponding constants of FixLs (BjFixL and RmFixL), EcDosH (*32*), and AxPDEAH (*31*). The O_2 association constants for all gas sensors, DevS and FixLs included, are considerably lower than for the globin family of proteins, represented by myoglobin and hemoglobin. O_2 dissociation rates for wild-type DevS and Y171F DevS are comparable. In both cases, O_2 dissociation rates are notably lower than for FixLs and globins. Only RmFixLH provided a similar k_{offO_2} value (6.8 s^{-1}) (*30*). Taken together, these data suggest that DevS proteins are more effective stores of O_2 than CO. The Y171F mutant has slightly increased affinity for both gases, roughly 3-fold, as compared to wild-type DevS.

DISCUSSION

Full-length DevS, one of the two kinases that control DevR phosphorylation, plays a key role in allowing *M. tuberculosis* to enter the dormant phase.

Table 2: Autoxidation Rates of the Truncated Proteins, DevS A GAF, and DevS A/B GAF, and the Full-Length Y171F DevS Mutant[a]

protein	k (h^{-1})	$t_{1/2}$ (h)
DevS A GAF	0.046	16.5
DevS A/B GAF	0.027	26.0
full-length Y171F DevS	0.012	73.6

[a] Rates were measured at 25 °C in phosphate buffer (50 mM) containing 1 mM EDTA and 200 mM NaCl.

In our previous work, wild-type full-length DevS was compared to Y171F DevS in terms of resonance Raman data, UV−visible spectra, and autophosphorylation behavior (Tables 4 and 5). Functional assays performed with wild-type DevS revealed that the ferrous unligated form has intermediate kinase activity, and ligand binding either further activates the kinase (CO and NO) or completely inactivates it (O_2) (*23*). Earlier work using the kinase domain of DevS by itself showed that the isolated kinase core is active (*33*). Therefore, the role of the GAF A and GAF B domains is to repress or enhance the activity of the DevS kinase as a function of ligand identity and the diatomic gas concentration. The Y171F mutant is only capable of discriminating between the presence and absence of ligands and is unable to distinguish among them. Y171F DevS is active in the ferrous unligated form (five-coordinate complex) and inactive in the ligand-bound form (six-coordinate complex with CO, NO, or O_2) (*23*).

These data indicate that the Tyr 171 side chain is critical for activation and repression of the kinase activity as well as for discrimination among ligands. Here we present the kinetic and autoxidation data of Y171F DevS and compare it to those of wild-type DevS to glean more insight into the role of this particular amino acid side chain as well as the biological role of DevS in *M. tuberculosis* infections.

Previous resonance Raman studies established that the CO complexes of wild-type DevS exist as two conformers: the hydrogen-bonded conformer defined by the high correlation point at 1936 and 524 cm^{-1} in the plot of ν(C−O) versus ν(Fe−CO) and the non-hydrogen-bonded conformer defined by the low correlation point at 1971 and 490 cm^{-1} (Table 5) (*21*, *22*).

These conformers were identified in the truncated versions of DevS; however, their proportion was altered as a function of truncation. Briefly, while in DevS A GAF the two conformers were present in roughly equal concentrations, in full-length DevS the non-hydrogen-bonded conformer predominates (85%). In

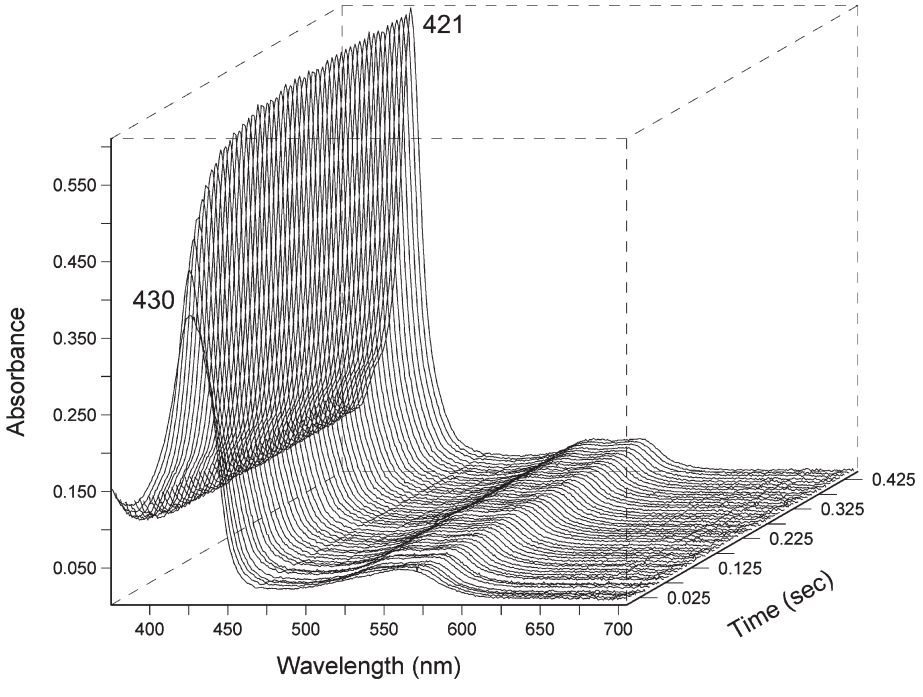

FIGURE 3: Representative traces of the binding of CO to Y171F DevS monitored in a diode array at 4 °C at 50 μM CO in the stopped-flow instrument.

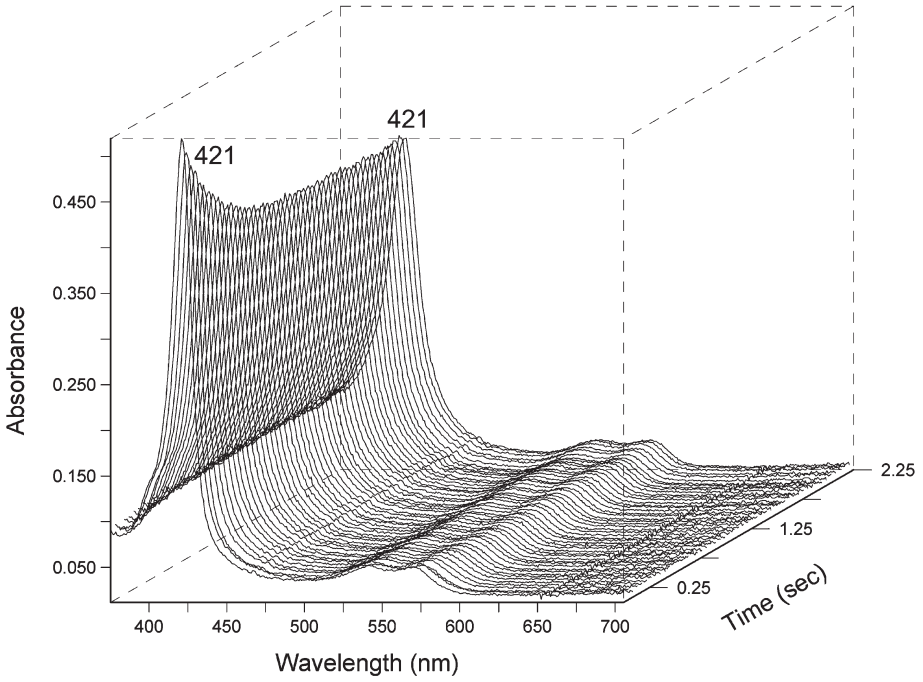

FIGURE 4: Representative traces of the CO displacement reaction of Y171F DevS Fe(II)CO with NO-saturated buffer, monitored in a diode array at 4 °C in the stopped-flow instrument.

Table 3: Summary of Kinetic Constants

protein	k_{on} (μM^{-1} s^{-1})	k_{off} (s^{-1})	K_d (μM)
	CO		
Y171F DevS	0.73 ± 0.071^a	2.43 ± 0.15^a	3.33
DevS	0.31 ± 0.031^a	2.57 ± 0.40^a	8.29
DevS A/B GAF	0.26 ± 0.024^a	2.45 ± 0.26^a	9.42
DevS A GAF	0.18 ± 0.007^a	2.74 ± 0.40^a	15.22
EcDosH (*32*)	0.0011	0.011	10
AxPDEAH (*31*)	0.21	0.058	0.28
BjFixL (*30*)	0.005	0.045	9
RmFixLT (*30*)	0.012		
RmFixLH (*30*)	0.017	0.083	4.9
	O_2		
Y171F DevS	32.4^b	3.85 ± 0.69^a	0.12
DevS	11.8^b	6.79 ± 0.33^a	0.58
EcDosH (*32*)	0.0026	0.034	13
AxPDEAH (*31*)	6.6	77	12
BjFixL (*30*)	0.145	20	138
RmFixLT (*30*)	0.217	11	51
RmFixLH (*30*)	0.217	6.8	31

[a] All other rates were determined in this work using the stopped-flow method. [b] The oxygen association constants were determined in this study using laser-flash photolysis.

Table 4: Summary of UV−Visible Spectra of Full-Length Y171F DevS and Wild-Type DevS

	Y171F DevS (*23*)			DevS (*21*)		
	γ (nm)	β (nm)	α (nm)	γ (nm)	β (nm)	α (nm)
Fe^{3+}	408	531	567	407	536	577
Fe^{2+}	430	561		428	559	
$Fe^{3+}NO$	420	534	568	419	534	568
$Fe^{2+}NO$	421	544	572	420	543	571
$Fe^{2+}CO$	421	538	569	422	538	566
$Fe^{2+}O_2$	422	538	570	414	541	576

DevS A/B GAF, the conformers are present in intermediate proportions (*22*).

Our kinetic analysis provides support for the existence of two conformers in the Fe^{2+} unligated complex of DevS, analogous to the two CO conformers detected by resonance Raman spectroscopy in the Fe−CO complex. In only one conformer, a hydrogen bond between the Tyr171 hydroxyl and a water molecule serves to position the water in the distal heme pocket in the proximity of the iron atom, however, not close enough to achieve coordination. Recently, the crystal structure of DevS A GAF was determined, confirming this conclusion (*20*). In the other conformer (for which structural or crystallographic data are lacking), no water molecule is fixed in the distal site at that position, resulting in unhindered access of the ligand to the heme iron. The absence of that "fixed" water molecule in the distal heme pocket can be interpreted as the result of the displacement of the Tyr171 side chain, its attachment point. Tyr171 may adopt a different conformation than in the crystal structures (*20*, *34*), where it serves as a gate that separates the immediate small distal heme pocket (10 $Å^3$) from a larger cavity of 45 $Å^3$; perhaps the phenol ring is flipped out of the way of the incoming ligand.

As the proportion of the hydrogen-bonded conformer of the Fe^{2+} unligated complex increases, the CO and O_2 association rates are expected to decrease. This trend was confirmed by the CO on rates determined in this study: DevS > DevS A/B GAF > DevS A GAF. In the case of the Y171F DevS mutant, no such hydrogen-bonded conformer can exist, and in fact, CO and O_2 association rates for Y171F DevS were roughly 3-fold higher than for full-length wild-type DevS, providing further support for this trend. The gas association rates for our DevS proteins suggest that interdomain interactions preferentially stabilize the conformer lacking the hydrogen-bonded water molecule.

We evaluated the stability of the oxy complexes of DevS and Y171F DevS in terms of autoxidation rates. Three recent papers have provided conflicting data on the autoxidation properties of

Table 5: Resonance Raman Vibrations of CO Complexes, with the Dominant Complex Shown in Bold

	H-bonded conformer		Non H-bonded conformer	
protein	ν(C−O) (cm^{-1})	ν(Fe−CO) (cm^{-1})	ν(C−O) (cm^{-1})	ν(Fe−CO) (cm^{-1})
Y171F DevS (*23*)	−	−	1965	497
DevS (*22*)	1936	524	1971	490
DevS A/B GAF (*22*)	1936	524	**1971**	**490**
DevS A GAF (*22*)	1936	524	**1971**	**490**

DevS. In 2007, Steyn et al. reported that their full-length DevS protein, isolated as a SUMO fusion, exists in the ferric form; the oxygen ferrous complex could not be isolated by the authors, and they concluded that it is completely unstable. On this basis alone, Steyn and co-workers concluded that DevS is a redox sensor (*19*). More recently, Cho et al. arrived at the same conclusion based on work done with the isolated GAF A domain of DevS (*20*). Yet another research group used a slow expressing vector to produce full-length DevS, and they reported an autoxidation half-life of 4 h at 37 °C (*18*). Our examination of the full-length DevS autoxidation behavior reveals that this heme protein actually forms a very stable oxy complex. The DevS autoxidation rates are extremely low under a variety of conditions. In the presence of K^+, Na^+, Mg^{2+}, and Ca^{2+}, ions that are universally present in biological fluids, DevS retains its stability, with autoxidation rates between 0.005 and 0.02 h^{-1}. Fe^{3+} increases the autoxidation rate to 0.09 h^{-1}, while Cu^{2+} accelerates the autoxidation reaction by 3 orders of magnitude to 25 h^{-1}, when present at the nonphysiological concentration of 0.1 mM. The high stability of the oxy−DevS complex establishes that this kinase acts as a gas rather than a redox sensor. This is consistent with DevS kinase activity being turned off upon oxygen binding to the ferrous complex.

In fact, as shown in Table 6, DevS is one of the most stable heme proteins. DevS is much more stable than the oxygen sensors EcDos and FixL; the DevS autoxidation rate is between 30 and 240 times lower. In addition, DevS is more stable than the human α- and β-hemoglobin chains and sperm whale myoglobin (SWMb); its stability at the physiological pH is comparable to that of bovine myoglobin under basic conditions (63 h half-life at pH 9).

In DevS, the heme moiety is associated with a GAF domain, whereas in all the other oxygen sensors in Table 6, including the *E. coli* phophodiesterase EcDos and the FixL kinases, the heme group is anchored in a PAS domain. This comparison suggests that the GAF protein fold is better able to stabilize the oxygen-bound heme against oxidation than the PAS domain. From the previously characterized PAS oxygen sensors, only AxPDEA1 is fairly stable (autoxidation half-life of > 12 h).

The previous data also suggest that the globin fold encountered in proteins used for either oxygen transport (hemoglobins) or oxygen storage (myoglobins) is more efficient in preventing autoxidation of the heme iron than are the PAS domains.

In this work, we show that in DevS the GAF domain effectively shelters the heme from autoxidation, leading to properties similar to those of myoglobins. The GAF domain was only recently shown to bind heme (*21*, *35*). DosT GAF was the first heme binding GAF domain to be crystallized (*34*). DevS is thus similar to DosT, another protein possessing a GAF-anchored heme moiety that has been shown to possess enhanced stability against autoxidation (*18*, *19*) (unpublished results).

Table 6: Autoxidation Rates of Various Heme Proteins[a]

protein	k (h^{-1})	$t_{1/2}$ (h)
EcDos-PAS[b] (*47*)	0.3	2.3
EcDos-PAS R97A[b] (*47*)	570	0.0012
EcDos-PAS R97E[b] (*47*)	2760	0.00025
EcDos (*48*)	0.7	1
AxPDEA1[c] (*31*)		> 12
BjFixL[d] (*30*)	2.8	0.25
RmFixLT[d] (*30*)	1.9	0.37
RmFixLH[d] (*30*)	2.3	0.3
SWMb[d] (*49*)	0.06	12
SWMb H(E7)L[d] (*49*)	10.4	0.07
bovine Mb[e] (*50*)	0.01	63
human Hb chain α[f] (*51*)	0.05	13
human Hb chain β[f] (*51*)	0.09	7.8

[a] Where Mb is myoglobin, Hb is hemoglobin, and EcDos is the *E. coli* Dos. [b] At pH 8 and 25 °C. [c] At pH 8 in Tris buffer at 23 °C. [d] At pH 7 and 37 °C. [e] At pH 9 and 25 °C. [f] At pH 8 and 35 °C.

In the case of the myoglobins, the presence of a distal pocket hydrogen bond donor that stabilizes oxygen in the ferrous species and a water molecule in the met form correlates with a $\gamma_{met}/\gamma_{oxy}$ of > 1 (the ratio of molar absorptivities at the wavelengths corresponding to the Soret peak). Typically, the distal hydrogen bond donor is a histidine residue which confers these spectral characteristics, and its lack usually results in a lower $\gamma_{met}/\gamma_{oxy}$ of < 1 (*36*).

Replacement of this hydrogen-bonding residue with a hydrophobic amino acid results in an altered $\gamma_{met}/\gamma_{oxy}$ of < 1 and in a blue shift of the Soret band for the met form. The same characteristic changes were observed in the case of DevS: mutation of Tyr171 to Phe decreased the $\gamma_{met}/\gamma_{oxy}$ ratio from 1.37 for the wild type to 0.97 for the mutant. This was accompanied by a blue-shifted Soret band for the respective ferric species, as expected. The intensity and position of the Soret band are considered to be strongly influenced by the structure of the distal heme pocket and by the interaction between the heme group and the apoprotein (*37*). In our case, the ferrous−oxy complex of the mutant had a red-shifted Soret band at 422 nm as compared to the wild-type band at 414 nm (Table 5), suggesting that the oxygen molecule is coordinating to the heme iron in a different distal environment.

Mutation of other residues in the myoglobin distal pocket that increased lipophilicity resulted in decreased autoxidation rates (*26*). In our case, mutation of Tyr to Phe also increases the lipophilicity of the heme pocket and, due to the absence of the Tyr hydroxyl in the mutant, favors exclusion of solvent and/or water molecules. This, in turn, increases the stability of the oxy complex and accounts at least in part for its low autoxidation rate.

The full-length protein demonstrated an increased stability to autoxidation as compared to the truncated DevS A GAF and DevS A/B GAF. The presence of the second GAF domain and, additionally, the kinase core decrease susceptibility to autoxidation. The full-length Y171F mutant displays an autoxidation behavior similar to that of the wild type.

Interdomain interactions among the GAF A domain of DevS, GAF B, and the kinase core and possibly interdomain interactions resulting from DevS dimerization are hypothesized to decrease the flexibility of the GAF A domain and stabilize the conformation resistant to autoxidation. The hypothesis that interdomain interactions enhance stability of heme proteins

against autoxidation is not unprecedented. In fact, Kawano et al. studied the relationship between artificial multiple-domain myoglobins and their tendency to undergo autoxidation. They found that as the number of domains increased, autoxidation rates decreased. The authors hypothesized that poly-domain formation stabilizes oxygen storage and reduces autoxidation rates, and they concluded that the structural flexibility of the globin domain is restricted in their unusual poly-domain myoglobins (*25*). In addition, naturally occurring polymeric hemoglobins from *Barbatia lima* demonstrate higher stability and reduced autoxidation rates as compared to the simple dimers of the hemoglobin chains (*25*). Human hemoglobin is much more resistant to autoxidation than the isolated α- and β-chains, and interdomain contacts are hypothesized to be responsible for this differential stabilization of the human hemoglobin tetramer (*38*).

Heme proteins are typically maintained in their active reduced state by a reduction system. This is the case for both myoglobin (*39*) and hemoglobin (*40*). In fact, in the absence of a functional reduction system, myoglobin would exist entirely in its met form, which is physiologically useless. In erythrocytes, oxidizing compounds convert 1.5−3% per day of hemoglobin to methemoglobin, but in vivo the methemoglobin is present in less than 1% due to the activity of this reducing enzymatic system (*41*).

In this work, we determined that DevS can be quickly reduced by a physiological reducing system, the gene products of Rv0688 and Rv0763c, an endogenous *M. tuberculosis* ferredoxin reductase and ferredoxin pair. This system may provide reducing equivalents to DevS in *M. tuberculosis* in vivo and thus help to maintain this kinase in its reduced active form. It is known that ferredoxins are highly similar proteins (*42*). FdxA is upregulated upon entrance into dormancy (*10*, *13*). The expression of the Rv0763c gene was induced in the murine lungs during tuberculosis infection (*43*). Thus, either the gene product of Rv0763c or FdxA could support DevS reduction in vivo. In addition to the already hypothesized roles of FdxA in dormancy, FdxA may serve to maintain DevS in its functional state.

As mentioned earlier, the positioning of the Tyr171 residue side chain in the distal heme pocket determines the activation or repression of the kinase function in DevS. It has previously been shown that the hydrogen bond to the coordinated O_2 is different from the hydrogen bond formed with CO or NO in the active site (*22*). The hydrogen bond to oxygen is not sensitive to protein truncations, suggesting two possibilities. (1) Only one hydrogen-bonded O_2 conformer is present in all constructs (Figure 5), or (2) several hydrogen-bonded O_2 conformers are present but indistinguishable by resonance Raman spectroscopy. These data suggest that the DevS protein is able to accommodate formation of a hydrogen bond to the coordinating O_2 more easily than in the case of NO or CO. This results in apparently relaxed steric constraints for the hydrogen bond to the oxygen molecule serving as the sixth heme ligand, with the Tyr171 side chain positioned differently than in the CO and NO complexes. Thus, oxygen binds to both wild-type DevS and Y171F DevS and forms complexes of comparable stability, as determined by O_2 dissociation and autoxidation rates. The downstream effect is in both cases inactivation of the histidine kinase activity (*23*).

We hypothesize that a different mechanism is at work in Y171F DevS in stabilizing the oxy complex of the mutant. This mechanism that substitutes for the stabilizing effect of the O_2 hydrogen bond in the wild type is most likely the interaction between the heme-bound oxygen molecule and the phenyl edge of

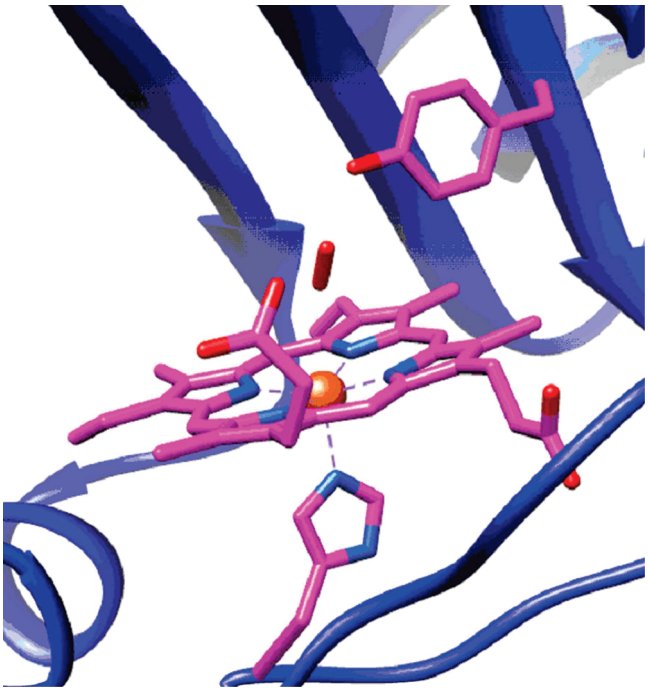

FIGURE 5: Model of oxygen binding to DevS A GAF based on the structure from the crystallized DevS A GAF (PDB entry 2W3F) (*20*) with the oxygen ligand positioned according to the DosT A GAF crystal structure (PDB entry 2VZW) (*34*). The porphyrin ring, His149, and Tyr171 are colored purple as capped sticks, while the protein backbone is represented as a blue ribbon. The oxygen molecule coordinating to the iron in the distal pocket is colored red.

F171. A large body of crystallographic data provides support for the favorable interaction between oxygen atoms bearing partial or integral negative charges and the edge of phenyl rings (*44*). Oxygen atoms from carbonyl groups (*44*) and negatively charged carboxylate oxygens (*45*) are frequently positioned at the edge of phenyl rings in proteins. This interaction is thought to be due in part to the electrostatic forces between the negative charge on the oxygen atom and the positive charge at the edge of the phenyl ring, which acts as a multipole having negative charge density below and above its surface. Another, perhaps more important, contribution is the polarization effect of the aromatic ring. In our case, the phenyl ring of F171 is hypothesized to interact with the partial negative charge on the oxygen atom. Heme-bound oxygen molecules are known to display superoxide character. This effect may be responsible for the stabilization of the Y171F oxy complex and correlates with its high stability to autoxidation and the low oxygen dissociation rate. This is analogous to the F29 oxymyoglobin mutant which displayed a higher stability to autoxidation and a lower oxygen dissociation rate than the wild-type protein. The crystal structure of F29 oxymyoglobin revealed a short distance of 3.2 Å between the bound oxygen molecule and the nearest carbon atom from the F29 residue; this suggested the presence of a favorable interaction between the oxygen partial negative charge and the positive edge of the phenyl ring (*28*).

The presence of partial negative charges in the distal pocket in the proximity of the bound ligand has been shown to destabilize the oxy complex in heme proteins, causing a decrease in the oxy complex stability of myoglobin mutants such as V68S and V68T (*26*). Partial negative charges present on the hydroxyl group from T68 in which the negative end of the T68 dipole

points toward the coordinating ligand have also been shown to increase the ν(C−O) frequency (*46*). The presence of the Y171 hydroxyl group in wild-type DevS may cause similar effects in terms of ν(C−O) stretching frequencies. The Y171 hydroxyl moiety in wild-type DevS is involved in hydrogen bonding to the ligand in one CO conformer [ν(C−O) = 1936 cm^{-1}], while in the other, the Tyr171 residue may adopt an entirely different conformation or its hydroxyl may orient itself with the negative end of its dipole toward the bound ligand giving the ν(C−O) of 1971 cm^{-1}. Removal of this partial negative charge in the Y171F DevS mutant results in a lower CO stretching frequency [ν(C−O) = 1965 cm^{-1}], and of course, the hydrogen-bonded conformer is entirely absent in this DevS mutant.

As a result, the distal heme pocket of the mutant provides only one CO conformer according to resonance Raman data, ν(C−O) at 1965 cm^{-1} and ν(Fe−CO) at 487 cm^{-1} (*23*) located close to the non-hydrogen-bonded conformer of DevS. In the DevS series, we therefore see a trend in autoxidation rates that is opposite from that of the myoglobin or hemoglobin models where hydrogen bonding stabilization between the distal His and bound CO corresponds to enhanced stability to autoxidation and higher correlation points on the ν(C−O) versus ν(Fe−CO) plots.

We conclude that the N-terminal GAF domain in full-length wild-type DevS effectively protects the ferrous oxygen-bound heme from oxidation under a variety of conditions. The presence of the most abundant cations, K^+, Na^+, Mg^{2+}, and Ca^{2+} ,does not decrease the stability of DevS. Two transition metal ions, Fe^{3+} and Cu^{2+}, enhance autoxidation 6- and >1000-fold, respectively, when present at 100 μM. However, in biological fluids, these ions are present at much lower levels.

The autoxidation properties of DevS clearly indicate that DevS functions as a gas sensor in vivo. Its stability to autoxidation is enhanced by interdomain interactions, and replacement of the key distal tyrosine with a phenylalanine residue results in a protein equally resistant to autoxidation.

ACKNOWLEDGMENT

We thank Hughes Ouellet for providing the ferredoxin (Rv0763c) and ferredoxin reductase (Rv0688) proteins and Dr. Wytze van der Veer for assistance with the laser-flash photolysis experiments.

SUPPORTING INFORMATION AVAILABLE

Time dependence of the reduction of DevS by an endogenous Mtb reducing system and the spectra before and after reduction of full-length DevS. This material is available free of charge via the Internet at http://pubs.acs.org.

REFERENCES

(1) World Health Organization (2006) Global tuberculosis control: Surveillance, planning, financing.
(2) Kochi, A. (1991) The global tuberculosis situation and the new control strategy of the World Health Organization. *Tubercle 72*, 1–6.
(3) Bloom, B. R., and Murray, C. J. (1992) Tuberculosis: Commentary on a reemergent killer. *Science 257*, 1055–1064.
(4) Kendall, S. L., Rison, S. C., Movahedzadeh, F., Frita, R., and Stoker, N. G. (2004) What do microarrays really tell us about *M. tuberculosis*?. *Trends Microbiol. 12*, 537–544.
(5) Wayne, L. G., and Hayes, L. G. (1996) An in vitro model for sequential study of shiftdown of *Mycobacterium tuberculosis* through two stages of nonreplicating persistence. *Infect. Immun. 64*, 2062–2069.
(6) Wayne, L. G., and Sohaskey, C. D. (2001) Nonreplicating persistence of *Mycobacterium tuberculosis*. *Annu. Rev. Microbiol. 55*, 139–163.
(7) Cunningham, A. F., and Spreadbury, C. L. (1998) Mycobacterial stationary phase induced by low oxygen tension: Cell wall thickening and localization of the 16-kilodalton α-crystallin homolog. *J. Bacteriol. 180*, 801–808.
(8) Ulrichs, T., and Kaufmann, S. H. (2006) New insights into the function of granulomas in human tuberculosis. *J. Pathol. 208*, 261–269.
(9) Seiler, P., Ulrichs, T., Bandermann, S., Pradl, L., Jorg, S., Krenn, V., Morawietz, L., Kaufmann, S. H., and Aichele, P. (2003) Cell-wall alterations as an attribute of *Mycobacterium tuberculosis* in latent infection. *J. Infect. Dis. 188*, 1326–1331.
(10) Sherman, D. R., Voskuil, M., Schnappinger, D., Liao, R., Harrell, M. I., and Schoolnik, G. K. (2001) Regulation of the *Mycobacterium tuberculosis* hypoxic response gene encoding α-crystallin. *Proc. Natl. Acad. Sci. U.S.A. 98*, 7534–7539.
(11) Yuan, Y., Crane, D. D., and Barry, C. E.III (1996) Stationary phase-associated protein expression in *Mycobacterium tuberculosis*: Function of the mycobacterial α-crystallin homolog. *J. Bacteriol. 178*, 4484–4492.
(12) Roupie, V., Romano, M., Zhang, L., Korf, H., Lin, M. Y., Franken, K. L., Ottenhoff, T. H., Klein, M. R., and Huygen, K. (2007) Immunogenicity of eight dormancy regulon-encoded proteins of *Mycobacterium tuberculosis* in DNA-vaccinated and tuberculosis-infected mice. *Infect. Immun. 75*, 941–949.
(13) Voskuil, M. I., Schnappinger, D., Visconti, K. C., Harrell, M. I., Dolganov, G. M., Sherman, D. R., and Schoolnik, G. K. (2003) Inhibition of respiration by nitric oxide induces a *Mycobacterium tuberculosis* dormancy program. *J. Exp. Med. 198*, 705–713.
(14) Roberts, D. M., Liao, R. P., Wisedchaisri, G., Hol, W. G., and Sherman, D. R. (2004) Two sensor kinases contribute to the hypoxic response of *Mycobacterium tuberculosis*. *J. Biol. Chem. 279*, 23082–23087.
(15) Dasgupta, N., Kapur, V., Singh, K. K., Das, T. K., Sachdeva, S., Jyothisri, K., and Tyagi, J. S. (2000) Characterization of a two-component system, devR-devS, of *Mycobacterium tuberculosis*. *Tuberc. Lung Dis. 80*, 141–159.
(16) Lee, B. Y., Hefta, S. A., and Brennan, P. J. (1992) Characterization of the major membrane protein of virulent *Mycobacterium tuberculosis*. *Infect. Immun. 60*, 2066–2074.
(17) Saini, D. K., Malhotra, V., and Tyagi, J. S. (2004) Cross talk between DevS sensor kinase homologue, Rv2027c, and DevR response regulator of *Mycobacterium tuberculosis*. *FEBS Lett. 565*, 75–80.
(18) Sousa, E. H., Tuckerman, J. R., Gonzalez, G., and Gilles-Gonzalez, M. A. (2007) DosT and DevS are oxygen-switched kinases in *Mycobacterium tuberculosis*. *Protein Sci. 16*, 1708–1719.
(19) Kumar, A., Toledo, J. C., Patel, R. P., Lancaster, J. R., and Steyn, A. J. (2007) *Mycobacterium tuberculosis* DosS is a redox sensor and DosT is a hypoxia sensor. *Proc. Natl. Acad. Sci. U.S.A. 104*, 11568–11573.
(20) Cho, H. Y., Cho, H. J., Kim, Y. M., Oh, J. I., and Kang, B. S. (2009) Structural insight into the heme-based redox sensing by DosS from *Mycobacterium tuberculosis*. *J. Biol. Chem.* (in press).
(21) Ioanoviciu, A., Yukl, E. T., Moenne-Loccoz, P., and Ortiz de Montellano, P. R. (2007) DevS, a heme-containing two-component oxygen sensor of *Mycobacterium tuberculosis*. *Biochemistry 46*, 4250–4260
(22) Yukl, E. T., Ioanoviciu, A., Ortiz de Montellano, P. R., and Moenne-Loccoz, P. (2007) Interdomain interactions within the two-component heme-based sensor DevS from *Mycobacterium tuberculosis*. *Biochemistry 46*, 9728–9736.
(23) Yukl, E. T., Ioanoviciu, A., Nakano, M. M., Ortiz de Montellano, P. R., and Moenne-Loccoz, P. (2008) A distal tyrosine residue is required for ligand discrimination in DevS from *Mycobacterium tuberculosis*. *Biochemistry 47*, 12532–12539.
(24) Suzuki, T., Watanabe, Y. H., Nagasawa, M., Matsuoka, A., and Shikama, K. (2000) Dual nature of the distal histidine residue in the autoxidation reaction of myoglobin and hemoglobin comparison of the H64 mutants. *Eur. J. Biochem. 267*, 6166–6174.
(25) Kawano, K., Uda, K., Otsuki, R., and Suzuki, T. (2004) Preparation of artificial 2-, 3-, 4- and 8-domain myoglobins and comparison of their autoxidation rates. *FEBS Lett. 574*, 203–207.
(26) Brantley, R. E.Jr., Smerdon, S. J., Wilkinson, A. J., Singleton, E. W., and Olson, J. S. (1993) The mechanism of autooxidation of myoglobin. *J. Biol. Chem. 268*, 6995–7010.
(27) Wallace, W. J., Houtchens, R. A., Maxwell, J. C., and Caughey, W. S. (1982) Mechanism of autooxidation for hemoglobins and myoglobins. Promotion of superoxide production by protons and anions. *J. Biol. Chem. 257*, 4966–4977.
(28) Carver, T. E., Brantley, R. E.Jr., Singleton, E. W., Arduini, R. M., Quillin, M. L., Phillips, G. N.Jr., and Olson, J. S. (1992) A novel

site-directed mutant of myoglobin with an unusually high O_2 affinity and low autooxidation rate. *J. Biol. Chem. 267*, 14443–14450.
(29) Saini, D. K., Malhotra, V., Dey, D., Pant, N., Das, T. K., and Tyagi, J. S. (2004) DevR-DevS is a bona fide two-component system of *Mycobacterium tuberculosis* that is hypoxia-responsive in the absence of the DNA-binding domain of DevR. *Microbiology 150*, 865–875.
(30) Gilles-Gonzalez, M. A., Gonzalez, G., Perutz, M. F., Kiger, L., Marden, M. C., and Poyart, C. (1994) Heme-based sensors, exemplified by the kinase FixL, are a new class of heme protein with distinctive ligand binding and autoxidation. *Biochemistry 33*, 8067–8073.
(31) Chang, A. L., Tuckerman, J. R., Gonzalez, G., Mayer, R., Weinhouse, H., Volman, G., Amikam, D., Benziman, M., and Gilles-Gonzalez, M. A. (2001) Phosphodiesterase A1, a regulator of cellulose synthesis in *Acetobacter xylinum*, is a heme-based sensor. *Biochemistry 40*, 3420–3426.
(32) Delgado-Nixon, V. M., Gonzalez, G., and Gilles-Gonzalez, M. A. (2000) Dos, a heme-binding PAS protein from *Escherichia coli*, is a direct oxygen sensor. *Biochemistry 39*, 2685–2691.
(33) Saini, D. K., and Tyagi, J. S. (2005) High-throughput microplate phosphorylation assays based on DevR-DevS/Rv2027c 2-component signal transduction pathway to screen for novel antitubercular compounds. *J. Biomol. Screening 10*, 215–224.
(34) Podust, L. M., Ioanoviciu, A., and Ortiz de Montellano, P. R. (2008) 2.3 Å X-ray structure of the heme-bound GAF domain of sensory histidine kinase DosT of *Mycobacterium tuberculosis*. *Biochemistry 47*, 12523–12531.
(35) Sardiwal, S., Kendall, S. L., Movahedzadeh, F., Rison, S. C., Stoker, N. G., and Djordjevic, S. (2005) A GAF domain in the hypoxia/NO-inducible *Mycobacterium tuberculosis* DosS protein binds haem. *J. Mol. Biol. 353*, 929–936.
(36) Korenaga, S., Igarashi, J., Matsuoka, A., and Shikama, K. (2000) A primitive myoglobin from *Tetrahymena pyriformis*: Its heme environment, autoxidizability, and genomic DNA structure. *Biochim. Biophys. Acta 1543*, 131–145.
(37) Puett, D. (1973) The equilibrium unfolding parameters of horse and sperm whale myoglobin. Effects of guanidine hydrochloride, urea, and acid. *J. Biol. Chem. 248*, 4623–4634.
(38) Tsuruga, M., Matsuoka, A., Hachimori, A., Sugawara, Y., and Shikama, K. (1998) The molecular mechanism of autoxidation for human oxyhemoglobin. Tilting of the distal histidine causes nonequivalent oxidation in the β chain. *J. Biol. Chem. 273*, 8607–8615.
(39) Hagler, L., Coppes, R. I.Jr., and Herman, R. H. (1979) Metmyoglobin reductase. Identification and purification of a reduced nicotinamide adenine dinucleotide-dependent enzyme from bovine heart which reduces metmyoglobin. *J. Biol. Chem. 254*, 6505–6514.
(40) Ogasawara, Y., Funakoshi, M., and Ishii, K. (2008) Glucose metabolism is accelerated by exposure to t-butylhydroperoxide during NADH consumption in human erythrocytes. *Blood Cells Mol. Dis. 41*, 237–243.
(41) Bodansky, O. (1951) Methemoglobinemia and methemoglobin-producing compounds. *Pharmacol. Rev. 3*, 144–196.
(42) Ricagno, S., de Rosa, M., Aliverti, A., Zanetti, G., and Bolognesi, M. (2007) The crystal structure of FdxA, a 7Fe ferredoxin from *Mycobacterium smegmatis*. *Biochem. Biophys. Res. Commun. 360*, 97–102.
(43) Talaat, A. M., Ward, S. K., Wu, C. W., Rondon, E., Tavano, C., Bannantine, J. P., Lyons, R., and Johnston, S. A. (2007) Mycobacterial bacilli are metabolically active during chronic tuberculosis in murine lungs: Insights from genome-wide transcriptional profiling. *J. Bacteriol. 189*, 4265–4274.
(44) Thomas, K. A., Smith, G. M., Thomas, T. B., and Feldmann, R. J. (1982) Electronic distributions within protein phenylalanine aromatic rings are reflected by the three-dimensional oxygen atom environments. *Proc. Natl. Acad. Sci. U.S.A. 79*, 4843–4847.
(45) Jackson, M. R., Beahm, R., Duvvuru, S., Narasimhan, C., Wu, J., Wang, H. N., Philip, V. M., Hinde, R. J., and Howell, E. E. (2007) A preference for edgewise interactions between aromatic rings and carboxylate anions: The biological relevance of anion-quadrupole interactions. *J. Phys. Chem. B 111*, 8242–8249.
(46) Li, T., Quillin, M. L., Phillips, G. N.Jr., and Olson, J. S. (1994) Structural determinants of the stretching frequency of CO bound to myoglobin. *Biochemistry 33*, 1433–1446.
(47) Ishitsuka, Y., Araki, Y., Tanaka, A., Igarashi, J., Ito, O., and Shimizu, T. (2008) Arg97 at the heme-distal side of the isolated heme-bound PAS domain of a heme-based oxygen sensor from *Escherichia coli* (Ec DOS) plays critical roles in autoxidation and binding to gases, particularly O_2. *Biochemistry 47*, 8874–8884.
(48) Sasakura, Y., Yoshimura-Suzuki, T., Kurokawa, H., and Shimizu, T. (2006) Structure-function relationships of EcDOS, a heme-regulated phosphodiesterase from *Escherichia coli*. *Acc. Chem. Res. 39*, 37–43.
(49) Quillin, M. L., Arduini, R. M., Olson, J. S., and Phillips, G. N.Jr. (1993) High-resolution crystal structures of distal histidine mutants of sperm whale myoglobin. *J. Mol. Biol. 234*, 140–155.
(50) Shikama, K., and Sugawara, Y. (1978) Autoxidation of native oxymyoglobin. Kinetic analysis of the pH profile. *Eur. J. Biochem. 91*, 407–413.
(51) Poli, A. L., Moreira, L. M., Hidalgo, A. A., and Imasato, H. (2005) Autoxidation studies of extracellular hemoglobin of *Glossoscolex paulistus* at pH 9: Cyanide and hydroxyl effect. *Biophys. Chem. 114*, 253–260.